NUMERICAL STUDY OF FLAME/VORTEX INTERACTIONS IN 2-D TRAPPED VORTEX COMBUSTOR

by

Debi Prasad MISHRA *, Renganathan SUDHARSHAN, and Perumal Kumaresan EZHIL KUMAR

Combustion Laboratory, Department of Aerospace Engineering, Indian Institute of Technology Kanpur, India

Original scientific paper
DOI: 10.2298/TSCI111006162M

The interactions between flame and vortex in a 2-D trapped vortex combustor are investigated by simulating the Reynolds averaged Navier-Stokes equations, for the following five cases: (1) non-reacting (base) case, (2) post-vortex ignition without premixing, (3) post-vortex ignition with premixing, (4) pre-vortex ignition without premixing, and (5) pre-vortex ignition with premixing. For the post-vortex ignition without premixing case, the reactants are mixed well in the cavity resulting in a stable C shaped flame along the vortex edge. Further, there is insignificant change in the vorticity due to chemical reactions. In contrast, for the pre-vortex ignition case (no premixing); the flame gets stabilized at the interface of two counter rotating vortices resulting in reduced reaction rates. There is a noticeable change in the location and size of the primary vortex as compared to case (2). When the mainstream air is premixed with fuel, there is a further reduction in the reaction rates and thus structure of cavity flame gets altered significantly for case (5). Pilot flame established for cases (2) and (3) are well shielded from main flow and hence the flame structure and reaction rates do not change appreciably. Hence, it is expected that cases (2) and (3) can perform well over a wide range of operating conditions.

Key words: *trapped vortex, primary vortex, secondary vortex, cavity stabilized flame, vorticity*

Introduction

In recent days, trapped vortex combustor (TVC) is considered as an alternate to the existing swirl stabilized combustors. In contrast to the conventional combustors, TVC employ cavities placed externally [1] or internally [2] as the flame stabilizer. An optimally designed cavity traps a vortex which is spatially and temporally stable over a wide range of inflow conditions [2]. In order to trap a stable vortex, Little and Whipkey [3] proposed an optimal cavity aspect ratio based on the minimum drag condition on the after-body. However, the effect of mass injection into the cavity was not considered by Little and Whipkey [3] in their experiments. Cavity injection is important for combustion applications as it would enhance the interactions between the cavity and the mainstream flows [4, 5]. This cavity injection, besides reinforcing the trapped vortex [4-6] and controlling the local equivalence ratio [6, 7], may also alter the cavity

* Corresponding author; e-mail: mishra@iitk.ac.in

flow structure [7]. Hsu *et al.* [2] through their experiments, found that the results obtained by Little and Whipkey for passive cavity (no cavity injection) were valid for the active cavities (with cavity injection) as well.

Flame established in a TVC cavity is termed as a *pilot flame* and the flame established in the region between the cavities is termed as the *main flame*. As the pilot flame is very well shielded from the main flow, it remains stable even when subjected to high values of main flow velocities [1, 2, 7]. Under reacting flow conditions, Hsu *et al*. (1998) [2] observed very low overall lean-blow-out equivalence ratios for a wide range of annular air velocity. Followed by Hsu *et al.*, Katta and Roquemore [4] studied the effects of cavity injection on the flow dynamics and observed that mass injection into the cavity increased the optimum aspect ratio of the cavity and injection of small amounts of fluid into a non optimum cavity increased the unsteadiness of the flow [4]. Besides this, Sturgess and Hsu [5] measured the entrainment of mainstream air into the cavity and arrived at correlations between the mainstream and cavity flow momentum flux ratio on the entrainment. Stone and Menon [6], and Mishra and Sudharshan [7] numerically investigated fuel-air mixing in the axisymmetric and 2-D TVC respectively and found that higher annular flow rates enhance the turbulent mixing between fuel and air in both reacting and non-reacting conditions. Hendricks *et al.* [1] performed numerical and experimental studies on a 2-D sector rig of a TVC with external cavities, with high speed diffuser flow. The overall performance in terms of emissions, combustion efficiency and blow-out limits are estimated for different inlet conditions and are found to be better than a conventional swirl combustor. Hewett and Madnia [8] studied the interaction between flame and a laminar vortex ring under various initial conditions. Flame characteristics and the effect of chemical reactions and heat release upon the local flow field are analyzed and presented. Renard *et al*. [9] discussed the dynamics of flame vortex interactions under laminar and turbulent conditions which presents basic concepts of flame behavior and interaction with vortices.

From the overview of the literature on TVC, it is evident that most of all researchers focus on the engineering aspects such as performance, design and optimization. Flame stabilization is an important aspect in the case of gas turbine combustors where, the ignition timing plays a vital role. It is expected that the flame stabilized by the trapped vortex and well shielded from the mainstream flow makes the TVC more stable as compared to conventional combustors. The fuel-air mixture in the TVC cavity can be ignited either at the instant of injection of fuel and air into the cavity or after a sufficient time so that the fuel and air are well mixed and a stable vortex is trapped within the cavity. Based on the injection timing, the flame stabilized within the cavity may either reinforce the trapped vortex or deteriorate the trapped vortex in the cavity. The aim of the present investigation is to unravel the effect of ignition timing and role of premixing on the flame-vortex interactions. Hence, understanding of flame vortex interaction in the cavity is important for the performance of TVC under various operating conditions which is lacking in open literature. In the present work, efforts are devoted to study the effect of ignition timing and role of premixing on the flame-vortex interactions in a 2-D TVC. To carry out this investigation, we have considered five cases namely, (1) non-reacting (base case), (2) post vortex ignition with no-premixing, (3) post vortex ignition case with premixing, (4) pre vortex ignition case with no-premixing, and (5) pre-vortex ignition case with premixing. Cases (2) and (4) represent two different startup conditions and illustrate the relative benefit of one over the other. Cases (3) and (5) also represent two different start-up conditions, however with mainstream premixing. Through such cases, the effect of reacting conditions upon the cavity flow field and the flame characteristics are studied and presented.

The computational domain and the numerical procedure

The present simulation was based on the Reynolds averaged form of mass, momentum, and energy conservation equations [7, 10]. FLUENT v6.3.26 code was used to carry out the simulations to obtain an unsteady 2nd order accurate solution for both reacting and non-reacting flow cases. The PISO algorithm was used for pressure velocity coupling and power law scheme was used to discretize the momentum and turbulence transport equations. The turbulence-chemistry interaction was modeled using the eddy dissipation model (EDM) due to Magnussen and Hjertager [11]. The species transport equations were discretized by second-order upwind scheme. A brief discussion about the computational domain and the boundary conditions adopted in the present work and the turbulence and combustion models were provided in the subsequent sections.

The trapped vortex combustor and the computational domain

Figure 1 shows the schematic of a 2-D TVC with cavity injectors. The combustor has three sections: (1) the upstream section, (2) the cavity section, and (3) the downstream section as shown in fig. 1. The pilot flame stabilized in the cavity zone would ignite the incoming fuel-air mixture, resulting in the main flame. The 2-D computational domain with primary and secondary injection locations is shown in fig. 2. The TVC cavity can be characterized by a non-dimensional geometric parameter called the aspect ratio, which is the ratio of cavity length (L) to the depth (D). In the present case, the L/D ratio is maintained at 1.2. The work by Ahuja and Mendoza [12] states that flow in a rectangular cavity can be approximated as 2-D for $L/W < 1$, where W is the span of the combustor (in the z-direction). Hence in the present simulations, 2-D computational domain with unity span length is used as shown in fig. 2. It should be noted that all the cavity injections are made from slots located at the cavity aft wall such that a counter- stream wise vortex is established within the cavity [7]. The secondary air, fuel and primary air injectors are placed at locations $y/L_C \sim 0.1$, 0.2, and 0.25 from the origin (fig. 2).The secondary air

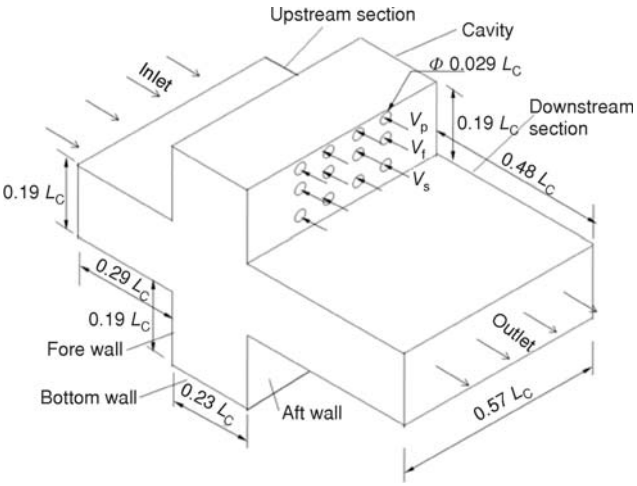

Figure 1. Schematic of the TVC showing different parts of the combustor

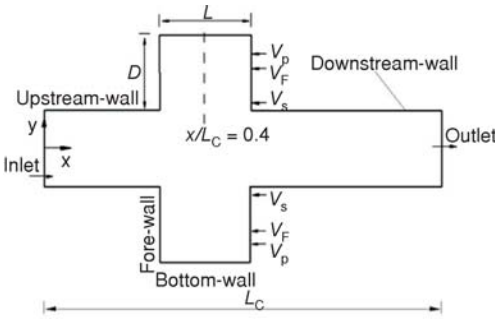

Figure 2. Computational domain of the TVC with fuel and air injection locations [7]

jet, fuel jet and the primary air jet are placed at locations $y/L_C \sim 0.11$, 0.2, and 0.25 respectively, where L_C is the length of the combustor. If the total length of the combustor is L_C, then cavity length, cavity depth, upstream length and downstream length are maintained at 0.23 L_C, 0.19 L_C, 0.29 L_C, and 0.48 L_C, respectively. Initially, the domain is meshed by maintaining $\Delta x = 0.75$ mm, $\Delta y = 0.57$ mm in the upstream section, $\Delta x = 0.625$ mm, $\Delta y = 0.57$ mm for the downstream section, $\Delta x = 0.5$ mm, $\Delta_y = 0.57$ mm for the interior and $\Delta x = 0.5$ mm, $\Delta y = 0.2$ mm for the cavity sections. With this grid size, the total number of mesh in the cavity domain is around 15,480. Subsequently, gradient based grid adoption technique is employed in the cavity zone to refine the grids further to 35435 cells after which the solution become grid independent [13].

Boundary conditions

The various boundary conditions adopted in the simulations were given below. For all the cases, mainstream Reynolds number, Re_{ms}, was maintained at 80810 and at the cavity, uniform velocity boundary conditions were employed with velocity magnitudes 50 m/s, 2 m/s, and 1 m/s for secondary air, fuel, and primary air jets. Gaseous methane ($\rho \sim 0.669$ kg/m^3) was used as the fuel. Besides this, the temperature and pressure of fuel and air at all inlets were maintained at 300 K and 101325 bar. No slip adiabatic boundary condition was used for the walls and outflow boundary condition was specified at the exit.

Turbulence and combustion modeling

The flow inside the TVC cavity is highly turbulent in nature with high level of unsteadiness [4]. This turbulent flow was modeled using shear stress transport (SST k-ε) model. In non-premixed flames, turbulence mixes the fuel and oxidizer into the reaction zones where they burn quickly [10]. In such cases, the combustion was approximated to be limited only by the turbulent mixing and not by the reaction kinetics [10]. In the present simulations, the turbulence-chemistry interaction model, based on the work of Magnussen and Hjertager [11], called the eddy-dissipation model (EDM) was used to model the single step methane chemistry. This model requires both fuel and oxidizer to be present along with turbulence or a patch of products, to initiate chemical reactions [10]. In the present computation, a patch of local carbon dioxide mass fraction of 0.1 in a narrow zone consisting 70 cells (3 mm ×3 mm size) was employed to initiate combustion in the trapped vortex cavity. For the pre-vortex ignition case, the patch was turned on from the beginning of the simulation (*i. e.* $t = 0$). For post-vortex ignition case, to begin with, a non-reacting flow calculation was being carried out for a sufficient period of time (in the present case, 4.4 s) such that there were no significant fluctuations in the cavity flow (see fig. 14). At this instant ($t = 4.4$ s), the patch was turned on to ignite the cavity flame. The simulations were continued till $t = 6$ s with a time step of 0.001 s, and the results are presented in the subsequent sections. For premixed cases, the finite-rate/eddy-dissipation model was used, where both the Arrhenius and eddy-dissipation reaction rates were calculated. The minimum of these two rates was taken as the net reaction rate. Once the flame was ignited, the eddy-dissipation rate was generally smaller than the Arrhenius rate, and the reaction was mixing-limited. Hence, in our simulations whenever mainstream premixing was included, the finite rate with eddy dissipation model was employed to simulate the turbulence chemistry interactions. More details of these models can be found in the references [7, 10, 11]. Besides this, Ezhil Kumar and Mishra [14] conducted a validation study to check the applicability of the SST k-w turbulence model and EDM combustion model in TVC environment and found that the flow field and flame predicted by these models matched reasonably well with the experiments. Since, gaseous methane

is used as fuel in the present simulations, soot particles may not be present in the domain and hence, the radiation from the flame is likely to be minimum. However, in future we are planning to include radiation modeling in the simulations.

Results and discussion

The reacting and non reacting flow simulations are carried out for five cases as shown in tab. 1a. In order to study the flame structure and behavior, reaction was initiated after a stable vortex was trapped within cavity, case (2), and along with vortex formation at $t = 0$, case (4). These two cases are compared with each other in terms of flow structure, vortex strength and its location, and effectiveness in fuel-air mixing. In order to observe the effect of chemical reaction on the cavity flow field, cases (2) and (4) were compared with the non-reacting base case, case (1). Further, the sensitivity of the cavity stabilized flame to mainstream conditions was explored by premixing the mainstream flow with fuel – cases (3) and (5). Besides this, details of various cases in terms of power level, average velocity, equivalence ratio, and mainstream Reynolds number are provided in tab. 1b.

Table 1a. Details of various cases considered for analysis. All cases were carried out for a mainstream $Re_{ms} \sim 80810$, cavity equivalence ratio $\Phi_c \sim 0.3$, and momentum flux ratio $MFR \sim 1.56$

Case	Reaction	Ignition	Mainstream premixing
1	NO	–	–
2	YES	Post vortex formation ($t > 0$)	No
3	YES	Post vortex formation ($t > 0$)	$\Phi_{ms} \sim 0.5$
4	YES	Pre vortex formation ($t = 0$)	No
5	YES	Pre vortex formation ($t = 0$)	$\Phi_{ms} \sim 0.5$

Table 1b. Details of velocities, power level and equivalence ratio for all cases considered in the present investigation

Case	Re_{ms}	V_s [ms^{-1}]	V_p [ms^{-1}]	$V_{f,c}$ [ms^{-1}]	PL_C [kW]	PL_{ms} [kW]	PL_o [kW]	Φ_c	Φ_{ms}	Φ_o
1	80810	50	1	0	0	0	0	0	0	0
2	80810	50	1	2	5.6	0	5.6	0.34	0	0.03
3	80810	50	1	2	5.6	84	89.6	0.34	0.5	0.49
4	80810	50	1	2	5.6	0	5.6	0.34	0	0.03
5	80810	50	1	2	5.6	84	89.6	0.34	0.5	0.49

Identification of flame and vortex location

It is important to identify the flame surface in the numerical flow field and define its location within the cavity. In this regard, the reaction rate was employed as the flame marker. The reaction rate and vorticity curves were plotted, as shown in fig. 3 to identify the flame location

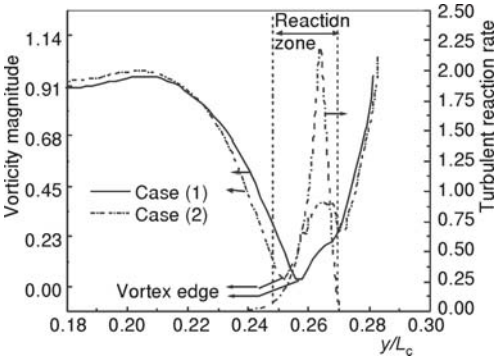

Figure 3. Vorticity magnitude and reaction rate plots along y-axis at $x/L_C = 0.4$

relative to vortex ring. In order to quantify flame location, 95% of peak reaction rate was marked as the *reaction zone* in the bell shaped reaction curve shown in fig. 3. It is equally important to locate the flame relative to the vortex ring; which in turn is required in identifying the location of the vortex edge. For this purpose, the vorticity magnitudes were also plotted with the reaction rate, along the y-axes as shown in fig. 3. It could be noted that the axis were chosen from the centre of primary vortex, extending towards the cavity walls. The vorticity magnitude which was inversely related to the core radius was plotted to identify the location of vortex edge. The plot in fig. 3 showed the vorticity magnitude dropping to a very low value (□1) from higher value in the core centre. The point of inflection in the vorticity curve was fixed as the vortex edge. The rise in the vorticity magnitude away from the vortex edge (outside the ring) was due to the presence of wall where vorticity was high because of localized recirculation zones. The vortex edge was located within the flame zone as indicated in the fig. 3. This suggested that the flame was anchored upon the vortex edge, which was expected to be the zone of very good mixedness. It was also observed that the location of vortex edge was slightly displaced under reacting conditions, as shown by the vorticity curve for the reacting case in fig. 3. This suggested that the vortex shrank in size due to the influence of chemical reactions and heat release. Finally, the vorticity curve for the reacting case, in contrast to the non-reacting case revealed a rise in the flame zone, as seen in the fig. 3. Hence there was generation of vorticity due to the presence of flame.

Flow characteristics and fuel-air distribution within the cavity

The non-reacting case was considered as the base case which was characterized by optimal values [13] of the momentum flux ratio (*MFR* = 1.56), aspect ratio (*L/D* = 1.2), and primary injection locations. The optimum value of *L/D* obtained from the earlier study [13] was in good agreement with the results of Hsu *et al.* [2]. Besides this, the same momentum flux ratio was reported to be effective with 25% mainstream entrainment into the cavity for the axisymmetric TVC [5]. As per the previous study [13], the base case was taken such that for an optimal value of the above mentioned parameters, a temporally and spatially stable vortex was trapped within the cavity that rolls up good amount of primary fuel and air rendering good mixing. For enhancement of mainstream entrainment into cavity, it was found that the momentum flux ratio of secondary to mainstream air must be greater than or equal to 1 [7, 13]. The solution was initially started without initiating reaction in the flow domain, in order to observe mixing. For case (1), the flow was characterized by a large centrally placed primary vortex and a smaller secondary vortex at the upstream top corner, as shown in fig. 4(a). Most of the primary air and fuel were rolled up in the primary vortex and the secondary vortex was found to be a region of lean fuel composition [7].

Post vortex ignition cases, case (2) and case (3) also resulted in cavity flow similar to case (1), which revealed that the cavity flow was least affected by the reaction for this case. It could be observed from fig. 4 that the flow along the shear layer got bifurcated at the vicinity of

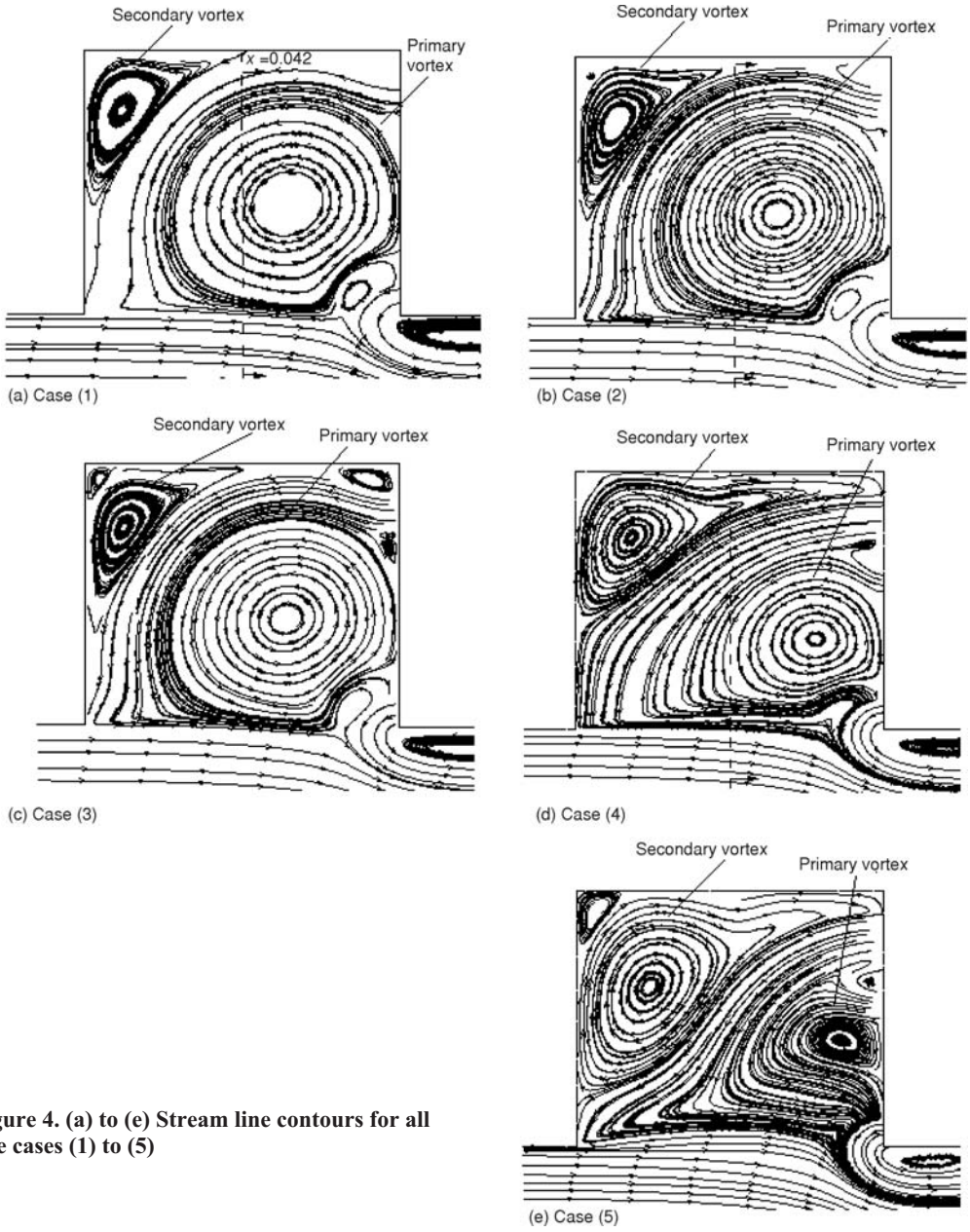

Figure 4. (a) to (e) Stream line contours for all five cases (1) to (5)

the secondary air injection point, transporting a major portion of the hot products out while entraining air into the cavity. In contrast to the post vortex ignition case, pre-vortex ignition cases resulted in different flow pattern. For the non-premixed, pre-vortex ignition case – case (4), the size of the secondary vortex got expanded, resulting in pushing down the primary vortex towards the shear layer – fig. 4(d). The size of the secondary vortex was further expanded for the pre-vortex ignition case with premixing, case (5), as observed from fig. 4(e).

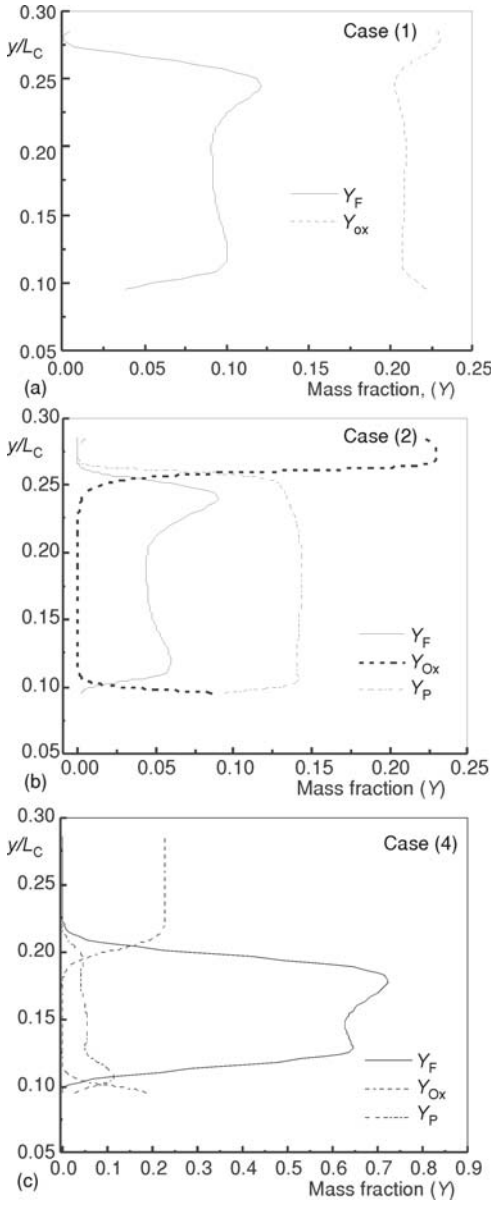

Figure 5. Mass fraction plots of fuel, oxidizer, and product for (a) case (1), (b) case (2), and (c) case (4)

The mass fraction plots along y/L_C at x/L_C ~ ~0.4 (as indicated in fig. 2) in the cavity for various cases were shown in fig. 5. It was observed form fig. 5(a) that both fuel and oxidizer were present together in the vortex core and their homogeneity in composition could be understood from the *flat* nature of curves (implying uniform composition) and hence indicated the well mixedness of the fuel/air mixture [6, 7, 15]. The hot products and any unreacted fuel were expected to be transported out of the cavity along the secondary jet which helps in igniting mainstream fuel-air mixture. This suggested that the vortex rolled up the incoming fuel and air (through primary injections) and distributed them uniformly across the cavity domain. For case (2), it could be observed that the fuel and oxidizer co-exist only at the vortex edge as shown in fig. 5(b). The fuel and oxidizer in the core region for case (1) was now replaced by products as shown in the fig. 5(b). The sharp gradient in the fuel, oxidizer and product concentrations in fig. 5(b) indicated the location of flame from first principles and this could be verified by the reaction rate plot shown in fig. 3. Hence, the flame was observed to be anchored and stabilized at the edge of the trapped vortex, which was an interface of the fuel and air jets entering the cavity domain where mixing was predominant. The flame consumed all the fuel present initially in the core and replaced them with products. As a result, a high temperature zone is likely to prevail within this zone.

The mass fraction plot for the pre-vortex ignition case, case (4), was shown in fig. 5(c). It could be observed from the plot, fig. 5(c) that the core region was occupied by fuel. The mass fraction plots in fig. 5(c) showed very high fuel concentration only towards the lower half of the cavity which was attributed to the lack of entrainment of primary air into the primary vortex caused by the developing flame. Similarly, fuel entrainment into the secondary vortex was also restricted by the flame. Hence, the cavity domain was characterized by two vortices: a primary vortex replete with fuel and a secondary vortex replete with oxidizer. The sharp gradients of reactant and product mass fractions were observed at the interface of the primary and secondary vortices as seen in fig. 5(c). Hence, the flame is anchored at the interface of two counter rotating

vortices unlike case (2) where it is anchored on a single vortex edge. Such a flame is expected to be less stable and more sensitive to mainstream conditions. This was caused due to the secondary vortex, which grew in size and rolled most of the primary air injected and leaving the primary vortex rich in fuel. This hampered the fuel-air mixing at the interface causing the flame to be stabilized in a comparatively narrow zone. This created a weakly stabilized flame that was highly sensitive to mainstream conditions. Also, due to the localized fuel accumulation and inefficient mixing, combustion is likely to be incomplete.

Flame-vortex interactions in the cavity

As mentioned in section *Identification of flame and vortex location*, a flame could be stabilized over the trapped vortex in the TVC cavity for certain operating conditions. However, it is not necessary that the flame will always be established over the trapped vortex. It should be noted that understanding of the flame and vortex stability is crucial for the better performance of the combustor as a whole. The nature of the flame and hence the cavity flow structure, in addition to the operating condition, may also depends on the ignition timing. This section is devoted to the study of the role of ignition timing on the interactions between the flow and flame within the TVC cavity.

Post-vortex ignition

This computation was started with initial data obtained from the solution of case (1). To study the effect of chemical reaction and temperature changes on flow field, the vorticity magnitude contours were shown for different cases, fig. 6(a) to (c). In fig. 6, the vorticity contours (shown by flood) are overlaid upon the reaction rate contours (shown by solid lines) to show location of flame in the cavity. It could be observed that the flame anchored along the vortex edge got attached with the shear layer flame at the cavity lip forming a *C* shaped flame as shown in fig. 6(b). As a result the core region

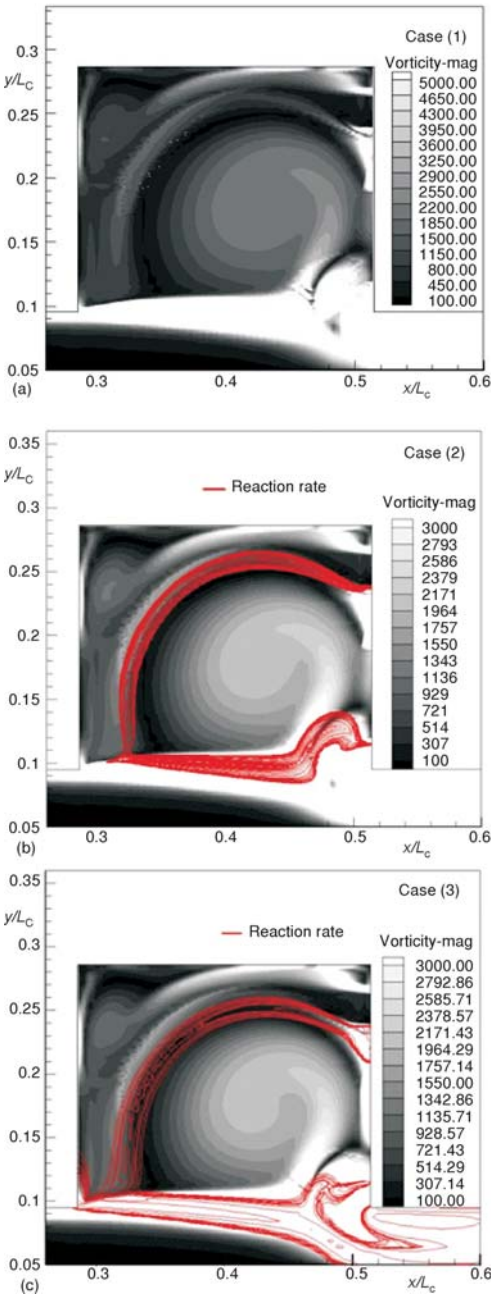

Figure 6. (a) Vorticity magnitude contour for case (1), (b) and (c) turbulent reaction rate contours overlaid upon vorticity magnitude contours for cases (2) and (3), respectively. Floods represent the vorticity contours while the solid lines (red colour) represent the reaction rate

was shielded by flame hampering the entrainment of primary air into it. This could be inferred from the mass fraction plot shown in fig. 5(b) that indicated very low oxidizer mass fraction in the core. In order to understand how the vorticity field was affected by the heat release, the vorticity contours for the reacting cases were compared with the non-reacting case in fig. 6(a). The cavity flow structure for case (1) and case (2) remained almost similar, which indicated that the heat release due to post vortex combustion is not altering the cavity flow structure. An attempt had been made to unravel the role of mainstream premixing on the flow and flame characteristics. Figure 6(c) showed the combined reaction rate and vorticity magnitude contour for post vortex ignition case with premixing, case (3). For this case, the reaction zone in the cavity got widened, besides the occurrence of reaction outside the cavity. The thickening of the reaction was due to the entrainment of mainstream fuel-air mixture into the cavity. From figs. 6(b) and (c), it could be concluded that though there was some changes in magnitude of the reaction rate (described in next subsection), the flame shape and location had not been significantly altered by mainstream premixing for these cases. The flame in this case was observed to extend towards the upstream corner of the cavity because flow separation at the corner creates a recirculation zone (which contains fuel because mainstream is premixed). From the above discussion, it was made clear that the cavity zone was not very sensitive to the main stream conditions and hence was well shielded from the main flow and the flame is likely to be stable for wider operating range.

In order to have a quantitative description of the flow and flame fields, the reaction rate (normalized by the maximum reaction rate) and the normalized vorticity magnitude were plotted along y/L_C (at the location $x/L_C \sim 0.4$) for cases (2) and case (3) in figs. 7 and 8. As observed from fig. 7, reaction occurred at two zones namely (a) the cavity zone and (b) the shear layer. The magnitude of the flame in the shear layer was much higher as compared to that in the cavity zone. Moreover, the reaction zone was located just adjacent to the vortex edge (fig. 7), which indicated the flame was stabilized over the vortex edge. Similar features were observed for the case (3) as well (fig. 8), however, the magnitude of the reaction rate was higher as compared to the case (2). Since the mainstream air was premixed for this case, the increase in the power level caused the change in reaction rate magnitude. It could be observed that the structure of vortex

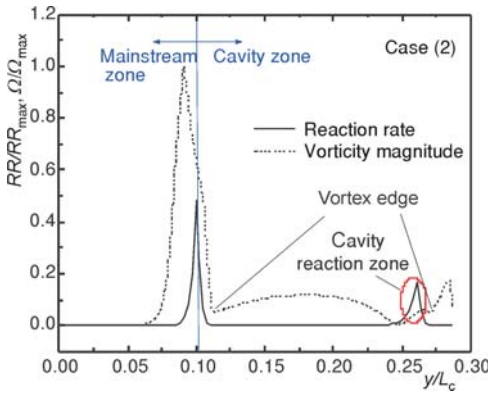

Figure 7. Normalized reaction rate and vorticity magnitude plot for post vortex ignition case without mainstream premixing at location $x/L_c = 0.4$

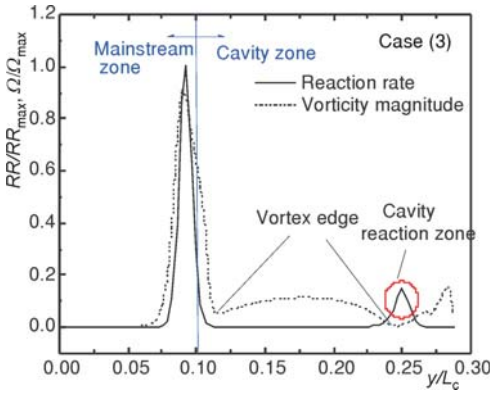

Figure 8. Normalized reaction rate and vorticity magnitude plot for post vortex ignition case with mainstream premixing at location $x/L_c = 0.4$

core for case (3) did not seem to undergo substantial change and their magnitude remained almost similar to that of case (2) as shown in fig. 8. This again demonstrated that the cavity field was well shielded from the mainstream flow and could remain stable for a wide range of operating conditions.

Pre-vortex ignition

In order to study the effect of flame on the developing vortex, reaction was initiated at $t = 0$ for case (4), unlike case (2) where, the solution was continued from the non reacting case. The combined contour plots of vorticity and reaction rate magnitude for case (4) and (5) were shown in fig. 9(a) and (b), respectively. In this case, there was re-location of the primary and secondary vortices as revealed in fig. 9(a). While the primary vortex was made to contract and propagate towards the downstream bottom corner, the secondary vortex expanded and extended well into the cavity zone in contrast to the non reacting case. The flame in this case lost the C shape and occured in a narrow zone between the two vortices and was relocated towards the downstream bottom corner as evident in fig. 9(a). From fig 9(a), it could also be observed that there was further reduction in vorticity magnitudes in the near-flame-region and the core region of the primary vortex, as compared to the post-vortex ignition case. This indicated stronger depletion of vorticity and hence greater influence due to chemical reactions for this case. The distortion in the flame shape (compared to case (2)) showed that the flame was not stabilized over the vortex edge. The reaction rate magnitudes were also observed to be lower compared to the post-vortex ignition case (explained in detail in next section). Similar observation was reported in the work of Hewett and Madnia [8]. This depletion is not conducive for combustion as it is likely to reduce the strength of the vortex and hence hampers flame stability. The mainstream premixing with fuel, case (5), had resulted in localized decrease in the vorticity magnitudes, as evident from fig. 9(b). The primary vortex had been made to shrink further and was sidelined towards the aft wall of the cavity. The flame was observed to be smeared along the shear layer, which rendered the primary vortex to shrink further (see fig. 9 (b)).

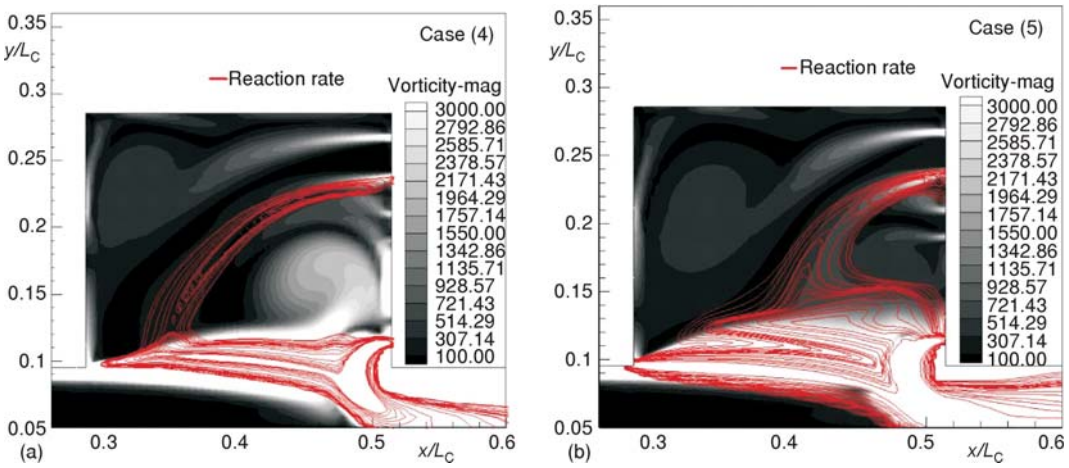

Figure 9(a) and (b).Turbulent reaction rate contours overlaid upon vorticity magnitude contours for pre-vortex ignition, cases (4) and (5), respectively. Floods represent the vorticity contours while the solid lines represent the reaction rate

Figures 10 and 11showed the normalized reaction rate and vorticity magnitude plots at the location $x/L_C \sim 0.4$ for case (4) and (5), respectively. The reaction rate magnitudes for the pre-vortex ignition cases were found to decrease considerably as compared to post vortex ignition cases. Moreover, the location of the peak reaction rate for case (5) was relocated considerably as compared to case (4). Hence, the reaction rate and vorticity contours were more vulnerable to mainstream conditions after the inclusion of mainstream premixing unlike case (3). Further, the reduction in magnitude of reaction rates compared to that of case (4) indicated that the flame was weak and highly sensitive to the mainstream flow. Overall, it was understood that the cavity flame is not well shielded from main flow and may not operate for wider range of operating conditions.

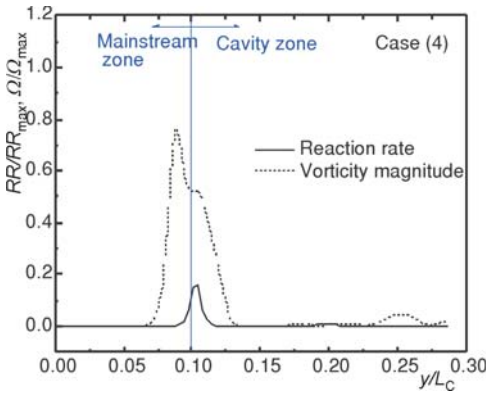

Figure 10. Normalized reaction rate and vorticity magnitude plot for case (4) at location $x/L_c = 0.4$

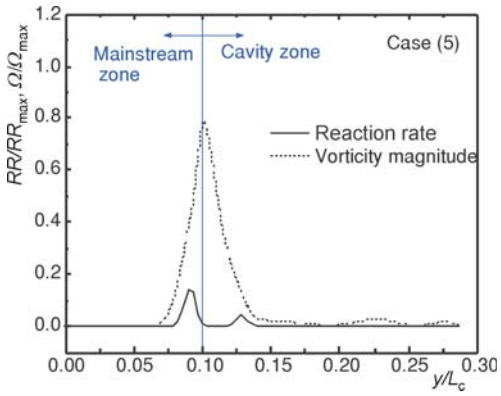

Figure 11. Normalized reaction rate and vorticity magnitude plot for case (5) at location $x/L_c = 0.4$

In order to visualize the effects of various operating conditions on the cavity flow field and reaction rate, the vorticity magnitude and reaction rate for all the cases were plotted together in fig. 12 and 13. It could be noted that the case (2) had higher vorticity magnitude as compared to case (1). The increase in vorticity magnitude was caused due to the generation of vorticity at the flame zone. Figure 12 also revealed that the vorticity magnitude of the pre-vortex ignition cases was being reduced by almost 25% in front of the flame (at corresponding locations) as compared to post vortex ignition cases. This indicated that there was depletion of vorticity which was expected to be due to the thermal stretching of flame at the vortex edge, similar to the observation made by Hewett and Madnia [8]. Since vorticity is a point variable, it provides only a local information and hence the flow field might be characterized by localized vorticity generation and depletion. Post vortex ignition case with premixing, case (3), resulted in almost 50% increase in the peak reaction rate magnitude at the shear layer. This was likely to occur as the power level of the main burner would increase with premixing. Interestingly, in the cavity domain, the peak reaction rate remained same with widening of the reaction zone. Entrainment of premixed fuel-air mixture in to the cavity by the secondary air jet was the cause for the widening of the cavity reaction zone. Besides this, there was almost 84% drop in the peak reaction rate magnitude for the pre-vortex ignition cases as compared to the post vortex ignition case. For these cases, the fuel was being ignited before being rolled up by the primary vortex. The lesser residence time for these cases might be also a reason for the lower values of reaction rate.

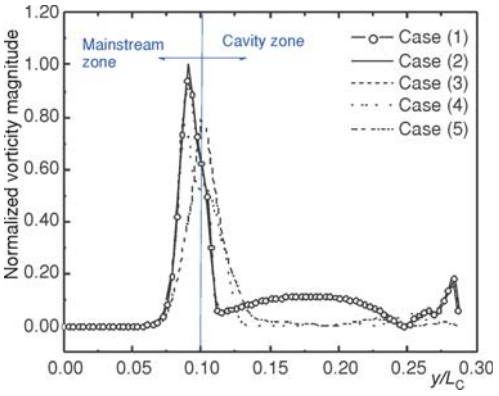

Figure 12. Normalized vorticity magnitude plot at location $x/L_c = 0.4$ for various cases

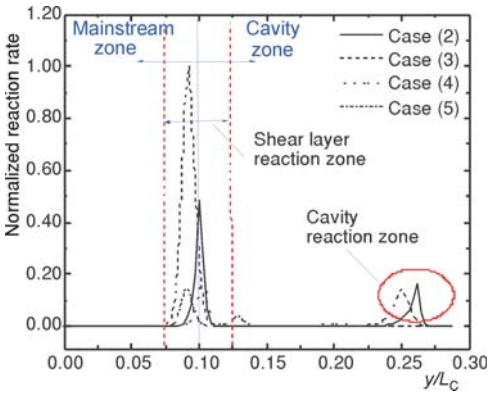

Figure 13. Normalized reaction rate plot at location $x/L_c = 0.4$ for various cases

Circulation in the cavity

In order to observe the effect of ignition timing on the cavity flow, the total circulation, Γ, within the cavity for various cases was plotted in fig. 14. The plot shown in fig. 14(b) indicated almost 100% increase in the circulation at $t = 4.56$ s (instant of ignition) which was caused due to the baroclinic production of vorticity. The initial peak in circulation was observed because of the forming vortex. Further, the mainstream premixing in case (3) resulted in a decrease in the vorticity magnitude near the flame location, as shown in fig. 12. The plots of Γ, fig. 14 (c) indicate that there was only a slight decrease in Γ after the mainstream was premixed with fuel. This suggested that the cavity zone was not very sensitive to the main stream conditions and hence was well shielded from the main flow and the flame is likely to be stable for wider operating range. The total circulation plot shown in fig. 14(e) indicated a 30% increase as compared to case (4). This is expected as there would be additional heat release occurring for case (5) in comparison to case (4). For both cases (4) and (5), it could be observed that there was an initial transient where the circulation was oscillatory after which it reached a steady state. This initial transient was caused due to the unsteadiness associated with the forming vortex that was coupled with the formation of flame.

Conclusions

The present numerical work was intended to characterize the interaction between flame and vortex in a 2-D trapped vortex combustor. For specific values of parameters like the mainstream Rems, momentum flux ratio, overall equivalence ratio and aspect ratio, the initiation of reaction was carried out at two different instances. In one case the flow field was allowed to develop forming a well mixed zone of fuel and air over a stable vortex within the cavity. On the other hand, reaction was initiated during the formation phase of the vortex. Initiation of the reaction during the post formation of the cavity vortex provided a stable flame along its edge. However, when reaction was initiated during the formation of the vortex, the interaction between flame and vortex becomes stronger. The flow field was characterized by two counter rotating vortices, where a weak flame was stabilized at the interface between the fuel rich and oxidizer rich vortices. There was a significant change in size and location of the primary vortex ring

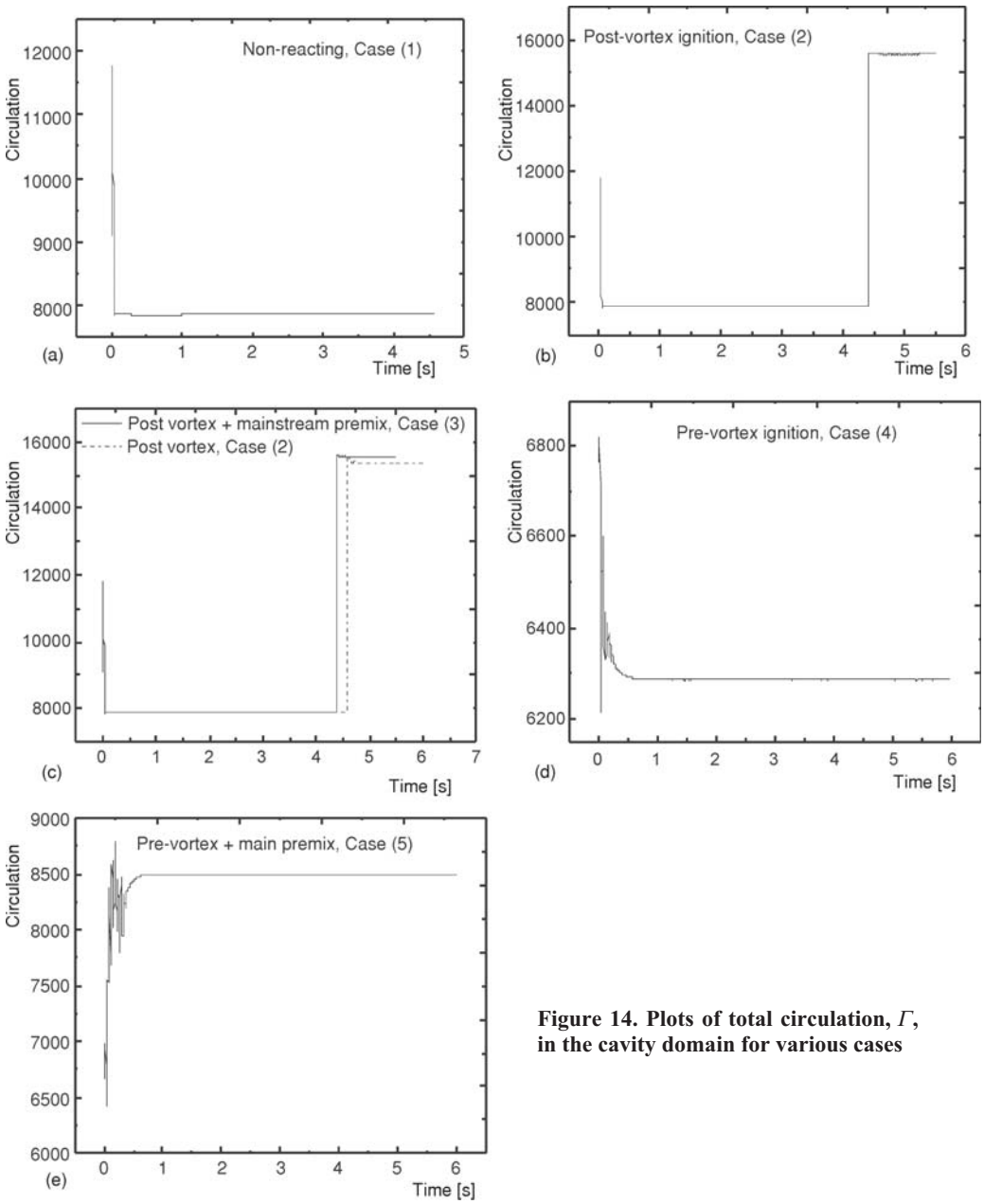

Figure 14. Plots of total circulation, Γ, in the cavity domain for various cases

as the vorticity magnitude diffused within the cavity. The reaction rates and peak vorticity magnitude plots of pre-vortex ignition case got reduced as compared to post-vortex ignition cases. Further, when the mainstream air flow was premixed with fuel the pre-vortex ignition produced a weak flame, whose enhanced interaction with the vortex resulted in further reduction in reaction rates and vorticity magnitudes. However, in the post-vortex ignition case, the reaction rate and vorticity magnitudes did not vary significantly. Hence a well protected cavity stabilized

flame was established which could render the TVC to perform optimally for wide range of operating conditions.

Nomenclature

D – depth of the cavity, [m]
L – length of the cavity, [m]
L_C – length of the combustor, [m]
MFR – momentum flux ratio, $[(\rho V^2)_c/(\rho V^2)_{ms}]$
PL_C – cavity power level, [kW]
RR – reaction rate
Re_{ms} – mainstream Reynolds number
V_{ms} – mainstream velocity, [ms^{-1}]
V_p – primary air velocity, [ms^{-1}]
V_F – fuel velocity, [ms^{-1}]
V_s – secondary air velocity, [ms^{-1}]
W – span of the combustor, [m]
x – variable distance along x-direction, [m]
y – variable distance along y-direction, [m]
Y_F – mass fraction of fuel
Y_{Ox} – mass fraction of oxidizer
Y_P – mass fraction of product

Greek symbols

Γ – circulation, [m^{2}s^{-1}]
Φ_c – cavity equivalence ratio
Φ_{ms} – main stream equivalence ratio
Φ_o – overall equivalence ratio
Ω – vorticity, [s^{-1}]

References

[1] Hendricks, R. C., *et al*., Experimental and Computational Study of Trapped Vortex Combustor Sector Rig with High-Speed Diffuser Flow, *International Journal of Rotating Machinery, 7* (2001), 6, pp. 375-385
[2] Hsu, K. Y., *et al*., Characteristics of a Trapped-Vortex Combustor, *Journal of Propulsion and Power, 14* (1998), 1, pp. 57-65
[3] Little, Jr B. H., Whipkey, R. R., Locked Vortex after Bodies, *Journal of Aircraft, 16* (1978), 5, pp. 296-302
[4] Katta, V. R., Roquemore, W. M., Study on Trapped Vortex Combustor – Effect of Injection on Flow Dynamics, *Journal of Propulsion and Power, 14* (1998), 3, pp. 273-281
[5] Sturgess, G. J., Hsu, K. Y., Entrainment of Mainstream Flow in a Trapped-Vortex Combustor, *Proceedings*, 35th Aerospace Sciences Meeting & Exhibit, Reno, 1997, Nev., USA, AIAA paper 97-0261
[6] Stone, C., Menon, S., Simulation of Fuel-Air Mixing and Combustion in a Trapped-Vortex Combustor, *Proceedings*, 38th Aerospace Sciences Meeting and Exhibit, Reno, 2000, Reno, Nev., USA, AIAA paper 2000-0478
[7] Mishra, D. P., Sudharshan, R., Numerical Analysis of Fuel-Air Mixing in a 2D Trapped Vortex Combustor, *Proceedings,* IMechE, Part G: *J Aerospace Engineering, 224* (2009), pp. 65-75
[8] Hewett, J. S., Madina, C. K., Flame-Vortex Interaction in a Reacting Vortex Ring, *Physics of Fluids, 10* (1998), 1, pp.189-205
[9] Renard, P. H., *et al*., Dynamics of Flame/Vortex Interactions., *Progress in Energy and Combustion Science, 26* (2000), 3, pp. 255-282
[10] ***, FLUENT® v6.3.26 Documentation, 1998
[11] Magnussen, B. F., Hjertager, B. H., On Mathematical Modeling of Turbulent Combustion with Special Emphasis on Soot Formation and Combustion, 16th Symposium on Combustion, Boston, Mass., USA, 1976, *Proceedings of the Combustion Institute,* Pittsburgh, Penn., USA, 1977, pp. 719-729
[12] Ahuja, K. K., Mendoza, J., Effects of Cavity Dimensions, Boundary Layer, and Temperature on Cavity Noise with Emphasis on Benchmark Data to Validate Computational Aero-acoustic Codes, NASA Contractor Report, No. 4653, 1995
[13] Sudharshan, R., Numerical Analysis of a 2D Trapped Vortex Combustor, M. Tech. thesis, Indian Institute of Technology, Kanpur, India, 2008
[14] Ezhil Kumar, P. K., Mishra, D. P., Numerical Modeling of an Axisymmetric Trapped Vortex Combustor, *International Journal of Turbo and Jet Engines, 28* (2011), pp 41-52
[15] Brodkey, R. S., *Turbulence in Mixing Operations: Theory and Application to Mixing and Reaction*, Academic Press, London, 1975

Paper submitted: October 6, 2011
Paper revised: June 27, 2012
paper accepted: September 15, 2012